

# Aggregation Modulators Interfere with Membrane Interactions of $\beta_2$ -Microglobulin Fibrils

Tania Sheynis,<sup>†§△</sup> Anat Friediger,<sup>†△</sup> Wei-Feng Xue,<sup>§</sup> Andrew L. Hellewell,<sup>§</sup> Kevin W. Tipping,<sup>§</sup> Eric W. Hewitt,<sup>§</sup> Sheena E. Radford,<sup>§\*</sup> and Raz Jelinek<sup>††\*</sup>

<sup>†</sup>Department of Chemistry and <sup>‡</sup>Ilse Katz Institute for Nanotechnology, Ben-Gurion University of the Negev, Beer-Sheva, Israel; and <sup>§</sup>Astbury Centre for Structural Molecular Biology and School of Molecular and Cellular Biology, University of Leeds, Leeds, United Kingdom

**ABSTRACT** Amyloid fibril accumulation is a pathological hallmark of several devastating disorders, including Alzheimer's disease, prion diseases, type II diabetes, and others. Although the molecular factors responsible for amyloid pathologies have not been deciphered, interactions of misfolded proteins with cell membranes appear to play important roles in these disorders. Despite increasing evidence for the involvement of membranes in amyloid-mediated cytotoxicity, the pursuit for therapeutic strategies has focused on preventing self-assembly of the proteins comprising the amyloid plaques. Here we present an investigation of the impact of fibrillation modulators upon membrane interactions of  $\beta_2$ -microglobulin ( $\beta_2$ m) fibrils. The experiments reveal that polyphenols (epigallocatechin gallate, bromophenol blue, and resveratrol) and glycosaminoglycans (heparin and heparin disaccharide) differentially affect membrane interactions of  $\beta_2$ m fibrils measured by dye-release experiments, fluorescence anisotropy of labeled lipid, and confocal and cryo-electron microscopies. Interestingly, whereas epigallocatechin gallate and heparin prevent membrane damage as judged by these assays, the other compounds tested had little, or no, effect. The results suggest a new dimension to the biological impact of fibrillation modulators that involves interference with membrane interactions of amyloid species, adding to contemporary strategies for combating amyloid diseases that focus on disruption or remodeling of amyloid aggregates.

## INTRODUCTION

The transformation of soluble proteins into amyloid fibrils deposited in different organs and tissues is a hallmark of devastating medical disorders, including Alzheimer's disease, Parkinson's disease, type II diabetes, and others (1,2). Although the presence of fibrillar aggregates appears to be a universal phenomenon in amyloid diseases, the relationships among amyloid formation, disease progression, and pathogenicity remain unclear.

Amyloid plaques are commonly found extracellularly, often associated with external membrane surfaces (3), although intracellular amyloid deposits are involved in several human disorders (3). A number of recent studies have linked the cytotoxicity of amyloid species with their membrane activity, suggesting that only toxic aggregates bind and disrupt lipid membranes, whereas benign conformers remain inert (4,5). There is an ongoing scientific debate, however, about the nature of pathogenic species. It was initially postulated that large insoluble amyloid plaques are the main culprits of the observed pathological conditions (6). This hypothesis was challenged by findings showing that small oligomeric intermediates, rather than the end-products of the aggregation pathway, represent the primary factors leading to cell damage and death (7,8). This concept

was taken further by the suggestion that rapid fibrillation may provide a protective mechanism through formation of inert deposits that reduce the population of transient oligomeric species (9). By contrast with these findings, several recent studies have implicated amyloid fibrils themselves in amyloid diseases. Specifically, fibrils derived from various amyloidogenic proteins have been shown to function as cytotoxic substances that readily bind and permeabilize lipid membranes (10–12), a process that is enhanced by fibril fragmentation (11,13). Preformed amyloid fibrils have also been shown to be internalized by cultured cells and to recruit cytosolic cellular proteins into growing amyloid assemblies (14). In vivo studies demonstrated that mature fibrils induce propagation of amyloidosis and the corresponding pathology in wild-type mouse (15) and human brains (16) through intercellular transmission. Finally, fibrils can be regarded as a source of toxic entities capable of releasing oligomeric species (17), particularly during interaction with lipids (18).

Directly related to the above observations, the mechanistic aspects of amyloid-protein interactions with cellular membranes have been the focus of intense experimental work in recent years (19,20). However, whereas lipid- and membrane-interactions of misfolded proteins appear to be closely related to amyloid cytotoxicity (4,5), development of therapeutic remedies has been directed in a large part toward substances that interfere with the aggregation processes of amyloid precursors into higher-order oligomeric species. Aggregation inhibitor screens have resulted in the discovery of numerous and diverse molecular leads, some

Submitted March 15, 2013, and accepted for publication June 4, 2013.

<sup>△</sup>Tania Sheynis and Anat Friediger contributed equally to this work.

\*Correspondence: [s.e.radford@leeds.ac.uk](mailto:s.e.radford@leeds.ac.uk) or [razj@bgu.ac.il](mailto:razj@bgu.ac.il)

Wei-Feng Xue's current address is School of Biosciences, University of Kent, Canterbury, Kent CT2 7NZ, UK.

Editor: Elizabeth Rhoades.

© 2013 by the Biophysical Society  
0006-3495/13/08/0745/11 \$2.00



of which have been shown to reduce amyloid-mediated cellular toxicity (21–23). Polyphenols, such as resveratrol (found in red grape skins and seeds) (24,25) and epigallocatechin gallate (EGCG, a component of green tea) (26,27) have been among the most widely studied inhibitors of amyloid cytotoxicity and fibril assembly modulators. These molecules have been shown to remodel toxic oligomers into large nontoxic aggregates (28–30) as well as to promote fibril disassembly (29,30). Another group of fibrillation modulators includes glycosaminoglycans (GAGs), anionic polysaccharides widely expressed in different tissue types (31). Heparin, an abundant member of the GAG family (31), has been demonstrated to modulate the fibrillation route and the associated toxicity of various amyloidogenic sequences (32,33). In addition, ionic chelators (21,34), molecular chaperones (35),  $\beta$ -sheet breaking peptides (22), antibodies (23),  $\gamma$ -bodies (36), and polymeric nanoparticles conjugated to functional groups (34,37) have all been used to modulate the course of fibril assembly.

Despite the apparent relationship between membrane interactions of amyloid assemblies and cellular toxicity, the impact of aggregation inhibitors upon membrane activity and lipid-binding properties of amyloid species has been addressed only sparingly (25,38). Here we investigate the relationships among the effects of different polyphenols and the glycosaminoglycans heparin and heparin disaccharide on membrane interactions of amyloid fibrils formed *in vitro* from  $\beta_2$ -microglobulin ( $\beta_2$ m).  $\beta_2$ m, the noncovalently bound light chain of the MHC-class I complex (39), forms insoluble fibrillar amyloid aggregates that are intimately involved in progression of dialysis-related amyloidosis (11,40,41). Interestingly, recent studies have demonstrated that  $\beta_2$ m fibrils, rather than the monomeric protein, are highly membrane-active and putative toxic substances (11). Here, we focus on membrane interactions of short (weight average length <400 nm)  $\beta_2$ m fibrils formed by controlled fragmentation of their initially longer counterparts (11,13). In particular, we describe the effects of polyphenols including the widely-studied fibrillation modulators EGCG and resveratrol (42), as well as the synthetic dye bromophenol blue and a second group of compounds consisting of glycosaminoglycans heparin and its building subunit heparin disaccharide (43), upon membrane interactions of  $\beta_2$ m fibrils. Furthermore, we examine whether these two distinct classes of molecules exhibit different effects upon membrane interactions of these fibrils.

## MATERIALS AND METHODS

### Materials

Chicken egg PC (L- $\alpha$ -phosphatidylcholine), chicken egg PG (L- $\alpha$ -phosphatidylglycerol), and NBD-PE (1,2-dipalmitoyl-*sn*-glycero-3-phosphoethanolamine-*n*-(7-nitro-2-1,3-benzoxadiazol-4-yl), ammonium salt) were purchased from Avanti Polar Lipids (Alabaster, AL).

TMA-DPH (1-(4-trimethyl ammonium phenyl)-6-phenyl-1,3,5-hexatriene), Laurdan (6-dodecanoyl-2-dimethylaminonaphthalene), and TMR (5-(and-6)-carboxytetramethyl-rhodamine) were purchased from Molecular Probes (Eugene, OR).

Heparin from porcine intestinal mucosa (sodium salt, grade I-A), heparin disaccharide I-A (sodium salt), EGCG ((-)-epigallocatechin gallate,  $\geq 95\%$ ), bromophenol blue, and resveratrol ( $\geq 99\%$ ) were obtained from Sigma-Aldrich (St. Louis, MO). Polymeric chains of full-length heparin supplied by Sigma-Aldrich can range from 18 to 90 monomers (6–30 kDa), whereas the majority of the chains contain 51–57 monomers (17–19 kDa).

### Preparation of fibril samples

Fibrils of wild-type human  $\beta_2$ m were formed from recombinant protein as previously described in Xue et al. (11). Briefly, lyophilized protein was dissolved in a fibril growth buffer containing 10 mM monosodium phosphate and 50 mM NaCl, pH 2.0, and was syringe-filtered through a 0.2- $\mu$ m pore size filter. The protein concentration was adjusted to 120  $\mu$ M and the solution was seeded with 0.1% (w/w) of fragmented  $\beta_2$ m fibrils formed under the same conditions, followed by incubation at 25°C under quiescent conditions for 48 h. This procedure was shown to result in formation of long straight  $\beta_2$ m fibrils (11). A quantity of 500  $\mu$ L aliquots of the fibril suspensions was subsequently fragmented by stirring (1000 rpm, 25°C for 48 h) on a custom-made precision stirrer. Fragmented long straight fibrils exhibiting a weight average length of <400 nm (11,13) were used in all experiments. For confocal microscopy,  $\beta_2$ m monomers were labeled by TMR as described in the Supporting Material. TMR-labeled fibrils were prepared by mixing unlabeled and labeled monomers such that the final preparation contained 10% of TMR-bound monomer.

### Vesicle preparation

Vesicles consisting of egg PC and egg PG (1:1, molar ratio) were prepared in a liposome buffer (50 mM HEPES, 110 mM NaCl, 1 mM EDTA, 0.02% (w/v)  $\text{NaN}_3$ , pH 7.4) at 2-mM total lipid concentration.

#### Large unilamellar vesicles

Large unilamellar vesicles (LUVs) were prepared by extruding the lipid suspension through a 400-nm pore-size polycarbonate filter as described in the Supporting Material.

#### Giant vesicles

NBD-PE (0.04%, molar ratio) was added to the lipid mixture for giant vesicle (GV) visualization by confocal microscopy. GVs were prepared using a rapid evaporation method (44). A quantity of 500  $\mu$ L of aqueous phase containing the liposome buffer supplemented with 0.1 M sucrose was added to 200  $\mu$ L of lipid-containing solution in chloroform in a round-bottom flask, followed by brief vigorous mixing of the two phases by pipetting. The organic solvent was immediately removed in a rotary evaporator under reduced pressure (40 mbar) for 3 min at room temperature. The resulting vesicle solution exhibited a turbid appearance and was used on the day of preparation.

### Vesicle disruption experiments in the presence of small molecules and heparin

Aliquots from the fibril stock solution (120  $\mu$ M monomer equivalent concentration) were mixed with the vesicles and fibril-membrane interactions were assessed through various spectroscopy and microscopy techniques. In each experiment fibrils were incubated for 3 min with the required amount of the test compound in the liposome buffer before addition to the vesicles using a  $\beta_2$ m/test compound ratio of 1:0.4 (w/w) for GAGs

( $\beta_2m$ :heparin, heparin disaccharide) or 1:1 (w/w) for polyphenols ( $\beta_2m$ : EGCG, bromophenol blue or resveratrol). Stock solutions of the tested small molecules and heparin were prepared in the buffer used for liposome preparations except for resveratrol, which was dissolved in buffer/ethanol 2:1 (v/v). For the control experiments, corresponding amounts of freshly prepared  $\beta_2m$  monomer in the fibril-growth buffer, the fibril growth buffer alone, or buffer/ethanol 2:1 mixture were used.

## Microscopy imaging

Fibrils preincubated in the liposome buffer alone or with test compounds for 3 min as described above were diluted 10-fold into the vesicle suspension, yielding a 12  $\mu M$   $\beta_2m$  monomer equivalent concentration and 1.8 mM total lipid concentration at a final pH of 7.4. The images were obtained after 15-min incubation of the fibrils with the vesicles.

### Confocal microscopy

Egg PC/PG/NBD-PE (1:1:0.0008 molar ratio) GVs and TMR-labeled  $\beta_2m$  fibrils were placed on a glass-bottom Petri dish (MatTek, Ashland, MA) and imaged on an Axiovert 100M confocal laser scanning microscope (Carl Zeiss, Jena, Germany) using a 63 $\times$ /1.4 N.A. Plan Apochromat DIC oil immersion objective lens (Carl Zeiss). The NBD-PE fluorescent probe was excited with the 488-nm line of an argon laser, while TMR fluorescence was excited with argon-krypton laser at 568 nm. Long-pass (LP) filters LP 505 and LP 580 were employed for acquisition of NBD and TMR fluorescence, respectively.

### Cryo-TEM

A drop of a sample solution containing egg PC/PG (1:1) LUVs incubated with fibrils alone or in the presence of the different test compounds was deposited onto a transmission electron microscope (TEM) 300-mesh Cu grid coated with a holey carbon film (Lacey substrate; Ted Pella, Redding, CA). Vitrification was achieved using an electron microscopy (EM) Grid Plunger (Leica Microsystems, Buffalo Grove, IL). The samples were examined at  $-180^\circ C$  using a Tecnai 12 G2 TWIN TEM (FEI, Hillsboro, OR) equipped with a model No. 626 cold stage (Gatan, Warrendale, PA), and the images were recorded using a model No. 794 charge-coupled device camera (Gatan) at 120 kV in low-dose mode.

## Liposome dye release assay

LUVs were prepared from egg PC/PG (1:1) as described above, except that a buffered carboxyfluorescein (CF) solution (50 mM CF, 50 mM HEPES, 10 mM NaCl, 1 mM EDTA, 0.02% (w/v)  $NaN_3$ , pH 7.4) instead of liposome buffer was used. After the extrusion, the LUVs were washed three times with liposome buffer by centrifugation at 20,000  $g$  and resuspension to yield a stock solution of 0.5 mM total lipids. A quantity of 2.5  $\mu L$  aliquots of these LUVs was then diluted into liposome buffer and mixed with fibrils (with or without test compounds as described above) to obtain a total sample volume of 500  $\mu L$  and a final protein concentration (in terms of  $\beta_2m$  monomer equivalent) of 3  $\mu M$ . The vesicles are saturated by the  $\beta_2m$  fibrils under these experimental conditions because further increase of  $\beta_2m$  concentration does not affect the extent of LUVs leakage (11). Fluorescence emission of carboxyfluorescein at 517 nm was then recorded for 15 min using an excitation wavelength of 490 nm on a FL920 spectrofluorimeter (Edinburgh Instruments, Edinburgh, Scotland, UK). The percent leakage was calculated as

$$\% \text{ Leakage} = \frac{(I_{\text{sample}} - I_0)}{(I_{100} - I_0)},$$

where  $I_0$  is the fluorescence intensity of liposomes alone and  $I_{100}$  is the fluorescence intensity after addition of 10  $\mu L$  of Triton X-100 (final concentration 0.4% (v/v)), which results in complete vesicle disintegration.

## Fluorescence anisotropy

The fluorescence probe TMA-DPH was incorporated into egg PC/PG (1:1) LUVs at final concentration of 0.22% (molar ratio) by mixing the dye dissolved in tetrahydrofuran at 1 mg/mL with the vesicle stock (2 mM) and incubating for 30 min at room temperature. The organic solvent comprised 0.2% (v/v) of the LUV stock solution. Fibrils alone or reacted with different test compounds were combined with 2.5  $\mu L$  aliquots of egg PC/PG/TMA-DPH LUVs prediluted with liposome buffer to a total sample volume of 500  $\mu L$ . The final protein concentration was 3  $\mu M$  ( $\beta_2m$  monomer equivalent). TMA-DPH fluorescence anisotropy was measured at 431 nm using an excitation at 360 nm on a FL920 spectrofluorimeter (Edinburgh Instruments). Anisotropy values were automatically calculated by the spectrofluorimeter software. Standard deviation values were obtained from 10 repeats of the anisotropy scans. Changes in anisotropy values ( $\Delta$  anisotropy) were calculated by subtracting the data for control samples (vesicles with the fibril growth buffer or with the buffer containing the appropriate test compound) from the corresponding fibril-induced anisotropy values.

## Laurdan fluorescence assay

Laurdan probe was dissolved in chloroform and added to the egg PC/PG (1:1) lipid mixture at 0.5% molar ratio before evaporation of the organic solvent. LUVs were then prepared as described above at 2 mM total lipid concentration. A quantity of 2.5  $\mu L$  aliquots of egg PC/PG/Laurdan LUV stock solution was diluted by liposome buffer (pH 7.4) to a final sample volume of 500  $\mu L$ , followed by addition of  $\beta_2m$  fibrils alone or preincubated with different test compounds at the ratios described above. The final protein concentration was 3  $\mu M$  ( $\beta_2m$  monomer equivalent). Laurdan emission spectra were recorded over a time course of 20 min using excitation at 365 nm on a PTI QuantaMaster spectrofluorimeter (Photon Technology International, Birmingham, NJ). Shift of emission maxima was quantified by general polarization (GP) function (45),

$$GP = \frac{(I_{\text{blue}} - I_{\text{red}})}{(I_{\text{blue}} + I_{\text{red}})},$$

where  $I_{\text{blue}}$  and  $I_{\text{red}}$  are emission intensities at 435 and 478 nm, respectively. Changes in GP values ( $\Delta$  GP) were calculated by subtracting the data for control samples (vesicles with fibril growth buffer or with the buffer containing the appropriate test compound) from the corresponding fibril-induced GP values.

## RESULTS

### Small molecules and heparin modulate fibril-induced membrane permeabilization

The molecules selected for this study belong to two families of well-known fibrillation modulators: polyphenols and glycosaminoglycans (GAGs) (Fig. 1). Specifically, plant-derived polyphenols EGCG and resveratrol were tested for their impact on fibril-membrane interactions, while the synthetic polyphenol bromophenol blue was employed for comparison with these natural compounds. The glycosaminoglycans heparin and heparin disaccharide (a minimal repeat unit of heparin (43) lacking its fibrillation-modulating activities (46)) were also examined. Heparin has been shown to affect amyloid formation of a peptide derived from the human prion protein, wherein aggregation was enhanced at low GAG/protein ratios and inhibited at higher heparin concentrations (46). In addition, heparin, but not its disaccharide,

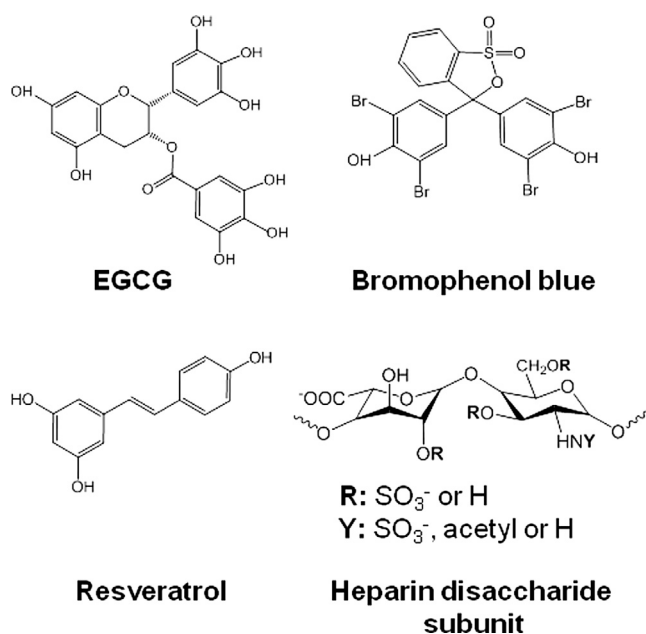


FIGURE 1 Molecular structures of the compounds studied. Note that both heparin polymer and its disaccharide subunit were used in the studies described.

has been shown to stabilize  $\beta_2m$  amyloid fibrils (47,48). The physical properties of the molecules used are summarized in Table 1.

Fig. 2 depicts dye release experiments designed to analyze permeation of large unilamellar vesicles (LUVs) composed of PC/PG (1:1) by  $\beta_2m$  fibrils, and the effect of the tested compounds upon the membrane disruption processes. The leakage experiments employed vesicle-encapsulated carboxyfluorescein, which initially is weakly fluorescent due to self-quenching at high concentration (49). After vesicle disruption by membrane-active analytes, dye leakage results in increased fluorescence emission. The experiments depicted in Fig. 2 A (*long dash*) confirm that the  $\beta_2m$  fibrils created in vitro interact with lipid membranes and induce membrane defects permeable for the water-

TABLE 1 Physical properties of molecules used in this study (61)

Compound	pK <sub>a</sub>	Log <sub>D</sub> , pH 7	Log <sub>P</sub>	Hydrogen bonds	
				Donors	Acceptors
EGCG	7.75 ± 0.25	0.57	0.639 ± 0.702	8	11
Bromophenol blue	4.12 ± 0.10	5.10	9.171 ± 1.046	2	5
Resveratrol	9.22 ± 0.10	3.02	3.024 ± 0.267	3	3
Heparin disaccharide	—	—	—	2–6	12–24

Log<sub>P</sub> is a partition coefficient of nonionized molecule between octanol and water; Log<sub>D</sub> is octanol/water partition coefficient of ionized and neutral species of a compound formed at a given pH. Total number of hydrogen bonds in a molecule corresponds to the number of hydrogen acceptors. All data are given for 25°C.

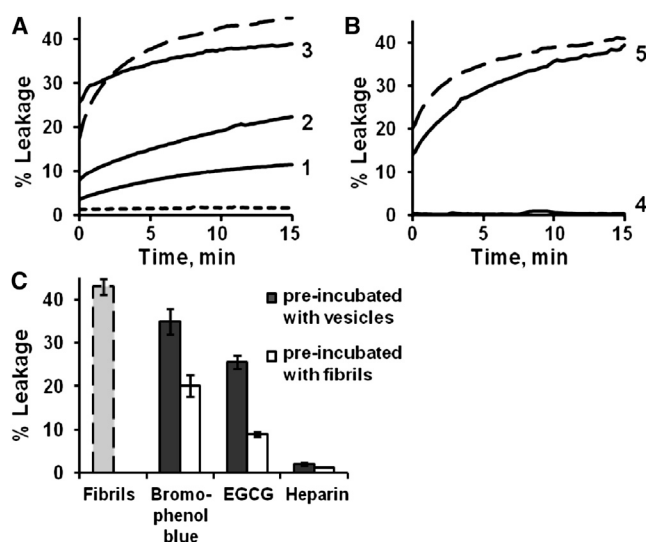


FIGURE 2 The effect of polyphenols and GAGs on  $\beta_2m$  fibril-induced vesicle leakage. Time-dependent increase in fluorescence reflecting leakage of carboxyfluorescein from PC/PG (1:1) LUVs after incubation with  $\beta_2m$ . (A) Effects of polyphenols on fibril-induced dye-leakage. (*Long dash*)  $\beta_2m$  fibrils alone (no fibrillation modulators added); (*short dash*)  $\beta_2m$  monomers alone; (1–3)  $\beta_2m$  fibrils incubated for 3 min with (1) EGCG, (2) bromophenol blue, and (3) resveratrol. (B) Effects of GAGs on fibril-induced vesicle leakage. (*Long dash*)  $\beta_2m$  fibrils alone;  $\beta_2m$  fibrils incubated for 3 min with (4) heparin polymer; and (5) heparin disaccharide. (C) Effect of preincubation of vesicles with different additives on  $\beta_2m$ -fibril induced membrane leakage. (*Shaded*)  $\beta_2m$  fibrils alone. (*Solid*) Fibrillation modulators incubated with vesicles for 30 min before addition of fibrils. (*Open*) Fibrillation modulators incubated with  $\beta_2m$  fibrils for 3 min before addition to the vesicles. Percent leakage corresponds to the end-point of the kinetic curves (see Fig. S3 in the Supporting Material).

soluble fluorescent dye, consistent with previous results (11). The  $\beta_2m$  fibrils, however, do not induce complete vesicle disintegration as evident from only partial membrane leakage (Fig. 2 A). This effect can be ascribed to fibril self-association at neutral pH (50), which presumably reduces amount of the fibrils available for membrane binding. An additional factor that may limit dye release by the fibrils includes nonhomogeneous distribution of lipid compositions within vesicle population (51). Addition of  $\beta_2m$  monomers did not result in vesicle leakage (Fig. 2 A, *short dash*), underscoring the fact that the  $\beta_2m$  monomers do not damage the lipid bilayer, at least as judged at the concentrations and solution/lipid conditions used.

Preincubation of the  $\beta_2m$  fibrils with the three polyphenols analyzed here (at weight-equivalent concentrations) shows that the effect of EGCG and bromophenol blue on membrane disruption by the fibrils differs significantly from that of resveratrol. Specifically, both bromophenol blue and EGCG inhibit the effect of fibrils on membrane permeability, although not completely (Fig. 2 A, curves 1 and 2). Incubation of the fibrils with either EGCG or bromophenol blue for more prolonged periods did not enhance the inhibitory capacity of the polyphenols (see Fig. S1 in the Supporting Material). Resveratrol, on the other hand,

accelerates initial dye release by the fibrils, whereas the long-term extent of the vesicle leakage is slightly reduced (Fig. 2 A, curve 3) as compared with fibrils alone. This enhancement in the initial amplitude of membrane permeability can be ascribed to resveratrol-membrane interactions (52) that may alter lipid bilayer susceptibility to the  $\beta_2m$  fibrils. Indeed, binding of resveratrol to LUVs was verified by changes in anisotropy of lipid-incorporated TMA-DPH probe (data not shown).

Negative-stain EM confirmed that the general morphology of  $\beta_2m$  fibrils was not affected by incubation with the polyphenols for 5 min (see Fig. S2). EM images, however, could not rule out that subtle structural changes within the fibrils contributed to the observed effects of the molecules tested. The dye-leakage results suggest that bromophenol blue and EGCG disfavor the formation of bilayer lesions by the  $\beta_2m$  fibrils, whereas resveratrol appears to have no inhibitory effect on  $\beta_2m$  fibril-induced impairment of membrane integrity. Fig. 2 B similarly shows dramatic differences between the effects of full-length heparin (curve 4) and heparin disaccharide (curve 5) upon vesicle leakage induced by  $\beta_2m$  fibrils. Specifically, whereas interaction of full-length heparin with  $\beta_2m$  fibrils prevents lipid bilayer disruption by these protein aggregates, heparin disaccharide had minor effect on the ability of the fibrils to cause dye release from the vesicles (Fig. 2 B).

Polyphenols are relatively hydrophobic molecules that have been shown to interact with membranes *in vitro* (53) and *in vivo* (52). Accordingly, studies conducted on EGCG have shown that it can cross the blood-brain barrier (52) and interact with model membranes without forming pores in the bilayer (53). We also observed membrane activity of EGCG through an increase in anisotropy of the membrane-incorporated fluorescent probe TMA-DPH in the presence of this molecule (data not shown). To determine whether EGCG and bromophenol blue inhibit the membrane activity of  $\beta_2m$  fibrils via insertion of these molecules into the lipid bilayer and subsequent stabilization of the membrane, rather than by altering membrane-fibril interactions, the polyphenols were incubated with vesicles before the addition of  $\beta_2m$  fibrils. The results of these experiments (Fig. 2 C and see Fig. S3) showed that 30-min preincubation of the polyphenols with LUVs did not enhance their inhibitory activity. On the contrary, the ability of the polyphenols to impair fibril-induced dye-leakage was attenuated compared with preincubation of these molecules with  $\beta_2m$  fibrils. Further control experiments confirmed that the polyphenols did not induce any detectable dye-leakage in the absence of fibrils even after the 30-min incubation with vesicles (data not shown). These findings suggest that EGCG and bromophenol blue suppress association of the  $\beta_2m$  fibrils with the PC/PG lipid vesicles, presumably by sequestering their exposed hydrophobic regions. By contrast with the action of the polyphenols, full-length heparin showed complete inhibition of membrane permeabilization by the

fibrils. This effect occurred whether or not heparin was preincubated with vesicles or with the fibrils (Fig. 2 C), implying rapid binding of this molecule to  $\beta_2m$  fibrils.

### Fibril-induced lipid bilayer deformation and impact of fibril modulators

The vesicle dye-leakage experiments shown in Fig. 2 report on the permeability of the lipid bilayer after incubation with  $\beta_2m$  fibrils. To examine the effects of fibrils on the bilayer integrity, giant vesicles (GVs) composed of PC/PG (1:1) incorporating the fluorescent probe NBD-PE (*green*) were mixed with  $\beta_2m$  fibrils containing rhodamine-labeled monomer (*red*) (see Materials and Methods). Imaging of the samples using dual-color fluorescence confocal microscopy allows simultaneous analysis of vesicle deformation (such as shape change and bilayer perturbation), as well as the behavior and localization of the  $\beta_2m$  fibrils relative to the lipids. Representative images depicting the experiments are shown in Fig. 3, while quantification of the data is summarized in Fig. S4 and Table S1 in the Supporting Material. The images obtained reveal a smooth, round shape of the GV that is unperturbed after incubation with buffer or with monomeric  $\beta_2m$  (Fig. 3, A and B, respectively), consistent with previous results (11,54). Images of the fibrils in the absence of vesicles show evidence for extensive fibril clustering at the pH used (pH 7.4) (Fig. 3 C).  $\beta_2m$  fibrils formed at pH 2 tend to bundle through lateral association when transferred to a higher pH (50), presumably due to the reduced positive charge. The fluorescence images shown in Fig. 3 D, (i) and (ii), provide a striking visual depiction of the effects of  $\beta_2m$  fibrils that destroy the integrity of the GV, consistent with previous results (54). Furthermore, the  $\beta_2m$  fibril aggregates (displaying the red rhodamine fluorescence) are coated by a thin layer composed of disassembled lipids (exhibiting green fluorescence) that appear to be extracted from the damaged vesicles. The confocal microscopy images in Fig. 3 D thus reveal significant vesicle disruption, consistent with extensive leakage of carboxyfluorescein from LUVs prepared from the same lipid composition (Fig. 2).

The confocal microscopy images presented in Fig. 3, E–G, show the effect of preincubating the  $\beta_2m$  fibrils with EGCG, bromophenol blue, or resveratrol before their addition to the liposomes. The results show that EGCG impairs  $\beta_2m$ -membrane interactions, giving rise to less abundant vesicle destruction compared with GV incubated with  $\beta_2m$  fibrils alone (compare Fig. 3, E and D(ii)). Quantitative analysis assessing ~100 vesicles in each sample (see Table S1) demonstrated that EGCG reduced the extent of fibril-damaged GV by approximately five times from 65 to 12% (see Fig. S4). Preincubation of the fibrils with bromophenol blue also resulted in only moderate GV disruption (17% of damaged vesicles, see Fig. S4), with some vesicles remaining intact (Fig. 3 F and see Fig. S4). Note that

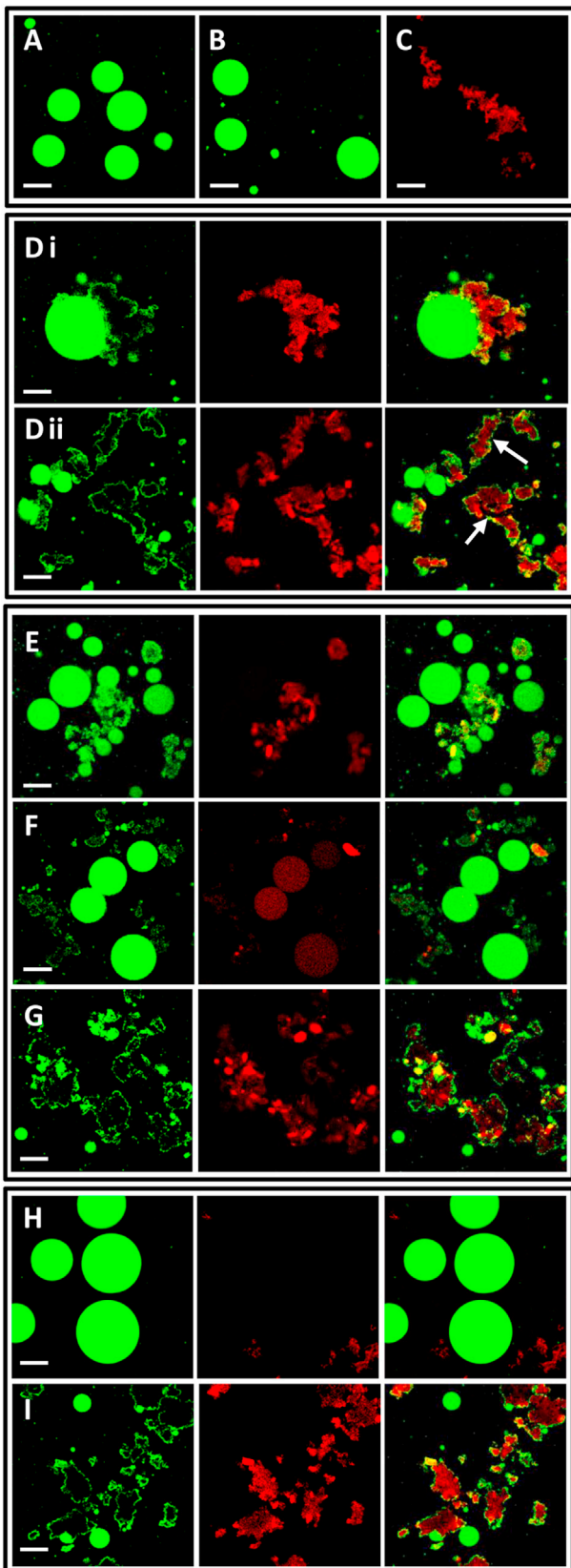


FIGURE 3 Confocal fluorescence microscopy employing liposomes containing NBD-PE (green) and  $\beta_2m$  fibrils labeled with TMR (red). (A) Control NBD-PE/PC/PG liposomes; (B) liposomes incubated with  $\beta_2m$  monomers; (C)

fluorescence intensity of the TMR probe is significantly quenched in the sample containing  $\beta_2m$  fibrils and bromophenol blue (Fig. 3 F), due to fluorescence resonance energy transfer between the emission spectrum of the fluorophore and the absorbance of the polyphenol. To visualize fibrillar aggregates in that sample, gain of the red channel has been increased, resulting in residual NBD signal to become visible as red fluorescence (Fig. 3 F).

In contrast with EGCG and bromophenol blue, which appear to suppress  $\beta_2m$ /vesicle interactions according to the confocal microscopy data, resveratrol does not show a significant effect on vesicle deformation caused by  $\beta_2m$  fibrils (Fig. 3 G and see Fig. S4), consistent with the finding that resveratrol is relatively inefficient in inhibiting  $\beta_2m$ -induced LUVs disruption as judged by the carboxyfluorescein dye release experiments (Fig. 2 A). The confocal images recorded after preincubation of the  $\beta_2m$  fibrils with heparin (Fig. 3 H) or heparin disaccharide (Fig. 3 I) highlight considerable difference between the impacts of these two compounds on the membrane activity of  $\beta_2m$  fibrils, corroborating the dye leakage results presented in Fig. 2 B. Accordingly, preincubation of the fibrils with the heparin polymer completely inhibited liposome disruption with no vesicle damage visible (Fig. 3 H and see Fig. S4). Binding of the full-length heparin to  $\beta_2m$  fibrils also resulted in the dispersion of the large fibrillar aggregates (Fig. 3 H) without alteration of the overall fibrillar appearance (see Fig. S2). Dispersed assemblies of the  $\beta_2m$  fibrils exhibit lower protein density and, as such, are not readily visible using fluorescence confocal microscopy. In sharp contrast with these results, heparin disaccharide did not inhibit vesicle damage by  $\beta_2m$  fibrils (Fig. 3 I and see Fig. S4), echoing the dye-leakage experiments presented in Fig. 2 B.

### Visualizing fibril-vesicle interactions using cryo-TEM

Cryogenic transmission electron microscopy (cryo-TEM) analysis can provide further visual depiction of the interactions of amyloid fibrils with lipid vesicles (54). This technique was used, therefore, to provide further insights into the effects of the polyphenols and GAGs on these interactions. Cryo-TEM images of LUVs created from PC/PG (1:1) are shown in Fig. 4 A. In the absence of fibrils, the lipid

TMR- $\beta_2m$  fibrils in pH 7.4 buffer. (D-I) (Left images) NBD-PE fluorescence (green); (middle) TMR fluorescence (red). (Right images) (D, i and ii) Superimposition. Liposomes incubated with TMR- $\beta_2m$  fibrils. (D(i) shows an example of a single, large liposome, enabling clear visualization of bilayer damage. (Arrows, D ii) Examples of fibrillar aggregates coated by lipids that were presumably derived from disintegrated vesicle(s). (E-I)  $\beta_2m$  fibrils preincubated with (E) EGCG, (F) bromophenol blue, (G) resveratrol, (H) heparin, or heparin disaccharide (I) before mixing with liposomes. Bars in all images correspond to 20  $\mu m$ . Note that residual NBD fluorescence is detected in the red channel of the image presented in panel F such that the NBD-labeled liposomes appear red.

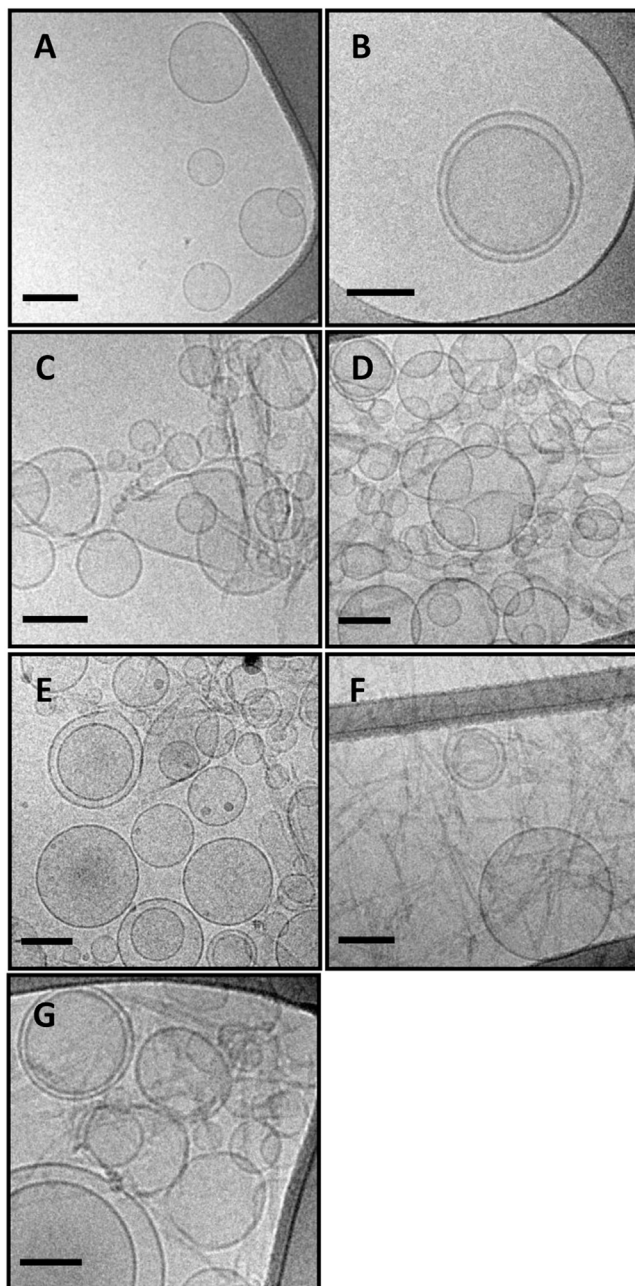


FIGURE 4 Cryo-TEM images of PGP LUVs treated with fibrils and different additives. (A) PC/PG (1:1) LUVs (control); (B) vesicles incubated with  $\beta_2m$  monomers; (C) vesicles incubated with  $\beta_2m$  fibrils; (D–G) preincubation of the  $\beta_2m$  fibrils with (D) EGCG; (E) bromophenol blue; (F) full-length heparin; and (G) heparin disaccharide before mixing with the vesicles. Bars in all images correspond to 100 nm.

vesicles do not adhere readily to an EM grid and hence only few vesicles are found in the control sample, with most of them located in the vicinity of the hydrophobic carbon mesh (Fig. 4 A). Vesicles treated with  $\beta_2m$  monomers appear spherical and undamaged, similar to the control sample (Fig. 4 B). Addition of  $\beta_2m$  fibrils to the vesicles gave rise to significant changes in liposome morphology and distribu-

tion (Fig. 4 C). Accordingly, vesicles visibly accumulated in the fibril-treated samples compared with images obtained of LUVs alone. Moreover, the vesicles appear to associate with the fibrils and to display significant perturbations to their otherwise round shapes, corroborating previous findings (54). Larger vesicles, in general, are more fragile than smaller ones, and therefore GV deformation caused by  $\beta_2m$  fibrils is more substantial (Fig. 3 D) than the changes to LUV shapes observed in Fig. 4 C. The cryo-TEM images in Fig. 4, D and E, show the effects of the addition of EGCG and bromophenol blue, respectively, on fibril-membrane interactions. These polyphenols appear to reduce vesicle deformation, consistent with the dye-leakage experiments and confocal microscopy images presented above. Indeed, in the presence of these small molecules, some vesicles remain free of fibrils and mostly retain their round shapes. The images of the heparin-treated fibril samples are even more striking (Fig. 4 F). In these images LUVs accumulation was not apparent and the vesicles appeared generally unperturbed in morphology. Heparin disaccharide, by contrast, had little effect on fibril-vesicle interactions; the image in Fig. 4 G features aggregated and distorted vesicles similar to the effects observed with the liposomes mixed with  $\beta_2m$  fibrils in the absence of this GAG.

#### The effects of fibril binding on lipid dynamics

To investigate further the effect of the  $\beta_2m$  amyloid fibrils on membrane bilayer properties and the consequence of preincubation with the fibril modulators, fluorescence anisotropy of PC/PG (1:1) LUVs that incorporate the fluorescence dye TMA-DPH was measured. The fluorescence anisotropy of TMA-DPH fluorophore, which is oriented perpendicular to the lipid bilayer plane (55), constitutes a sensitive probe for bilayer fluidity and dynamics (56). Fig. 5 A depicts the fluorescence anisotropy changes induced by  $\beta_2m$  fibrils and  $\beta_2m$  fibril/test compound mixtures upon addition to the TMA-DPH/PC/PG vesicles. The results revealed that incubating the vesicles with  $\beta_2m$  monomers did not alter the TMA-DPH anisotropy, consistent with the findings that  $\beta_2m$  monomers have no effect upon lipid membranes (Figs. 2–4).

By contrast, incubation of  $\beta_2m$  fibrils with the TMA-DPH/PC/PG vesicles gave rise to a pronounced increase in anisotropy (Fig. 5 A, ii), indicating reduced bilayer fluidity after binding of the membrane-active fibrils. The effect of bromophenol blue, heparin, and heparin disaccharide upon  $\beta_2m$  fibril-induced changes in TMA-DPH anisotropy are also depicted in Fig. 5 A, iii–iv (EGCG and resveratrol gave rise to a significant increase in TMA-DPH anisotropy when incubated with liposomes in the absence of fibrils, ruling out measurements of their effects on  $\beta_2m$ -induced changes of lipid dynamics). These experiments showed that preincubation of the fibrils with bromophenol blue substantially lowered  $\beta_2m$  fibril-induced

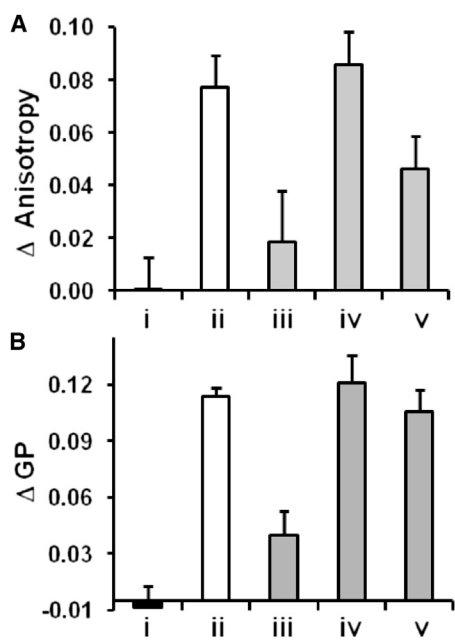


FIGURE 5 Modulation of bilayer fluidity by  $\beta_2m$  amyloid fibrils and different molecules. Changes in (A) fluorescence anisotropy of TMA-DPH and (B) Laurdan emission shift (quantified by GP, Materials and Methods) assayed within PC/PG (1:1) LUVs. The vesicles incubated with (i)  $\beta_2m$  monomers, (ii)  $\beta_2m$  fibrils, (iii–v)  $\beta_2m$  fibrils preincubated with (iii) bromophenol blue, (iv) full-length heparin, and (v) heparin disaccharide before mixing with the vesicles.

increase of lipid bilayer rigidity (Fig. 5 A, iii), consistent with inhibition of fibril-lipids interactions in the presence of this polyphenol.

Surprisingly, preincubating  $\beta_2m$  fibrils with full-length heparin did not attenuate the large increase in anisotropy observed when the fibrils were incubated with liposomes in the absence of any additives (Fig. 5 A, iv), despite the substantial evidence that heparin is able to protect LUVs and GVs from fibril-induced disruption. Thus, the anisotropy experiments suggest that heparin does not prevent the binding of the  $\beta_2m$  fibrils to the lipid bilayer, but instead interferes with the ability of the fibrils to cause bilayer disruption. Indeed, the cryo-TEM experiments depicted above indicate that association of heparin-coated  $\beta_2m$  fibrils with lipid vesicles appears to be attenuated (Fig. 4 F) relative to the binding of the untreated fibrils (Fig. 4 C). Accordingly, the image of the heparin/fibril mixture incubated with LUVs shows depletion of lipid vesicles (Fig. 4 F), consistent with impaired liposome-fibril interactions.

Addition of heparin disaccharide reduced the impact of the  $\beta_2m$  fibrils upon bilayer fluidity, as judged by TMA-DPH anisotropy, but to a lesser extent than was observed with bromophenol blue. The small heparin oligomer presumably interferes to some degree with membrane interactions of  $\beta_2m$ , but is not able to prevent bilayer disruption.

Changes in lipid bilayer fluidity after interactions with  $\beta_2m$  fibrils were also assessed using a different, comple-

mentary approach utilizing membrane-embedded Laurdan as a probe of lipid dynamics (Fig. 5 B). The fluorescence of Laurdan is sensitive to the polarity of the surrounding medium and thus is blue-shifted in more rigid lipid environments due to exclusion of water molecules from the probe proximity (45). The spectral shift is quantified using the general polarization (GP) function (45), which is proportional to the blue/red fluorescence ratio (Materials and Methods). The results in Fig. 5 B corroborate the TMA-DPH anisotropy data by demonstrating that  $\beta_2m$  fibrils induce an increase in GP values of Laurdan/PC/PG vesicles. This change in GP remained largely unaltered after preincubation of the  $\beta_2m$  fibrils with full-length heparin, reflecting a comparable reduction in lipid mobility in both cases (Fig. 5 B and see Fig. S5). Bromophenol blue, by contrast, largely blocked fibril-induced reduction of membrane fluidity, whereas heparin disaccharide exhibited marginal effect on fibril-lipid interactions. The  $\beta_2m$  monomer did not affect lipid bilayer dynamics, confirming that the monomeric protein is not membrane-active under the conditions employed here, consistent with the TMA-DPH anisotropy data.

## DISCUSSION

This study sheds light on an important question in the search for therapeutic solutions to amyloid diseases, namely the relationship between fibrillation modulators and the interactions of amyloid fibrils with membranes in the presence of these agents. Although the impact of inhibitors of amyloid formation on the aggregation pathways of amyloidogenic proteins has been studied extensively (27,29,57), the possibility that the same compounds may disrupt fibril-membrane interactions has not been investigated in depth before, to our knowledge. Here we focus on the interaction of in vitro-formed  $\beta_2m$  amyloid fibrils with PC/PG (1:1) lipid vesicles. We specifically chose  $\beta_2m$  fibrils for this study because these assemblies have been shown previously to be cytotoxic and to be capable of permeabilizing lipid membranes (11). Previous results have demonstrated that electrostatic interactions are important determinants that mediate membrane disruption by  $\beta_2m$  fibrils because increasing the fraction of negatively charged lipids within model membranes significantly enhances lipid bilayer permeabilization by these amyloid aggregates (11).

A recent study has revealed that interactions of fragmented  $\beta_2m$  fibrils with model membranes give rise to breakage or blebbing of the outer lipid leaflet, accompanied by appearance of small vesicles associated with the fibrils (54). These findings shed light on a possible mechanism by which  $\beta_2m$  fibrils elicit membrane permeabilization and disruption. Small lipid structures (presumably vesicles or micelles) have also been detected within other amyloid protein systems during the fibrillation process in the presence of LUVs (58). Furthermore, previous results have



shown that the formation of  $\beta_2m$  fibrils is not affected by the small molecules examined here (59), whereas heparin (but not heparin disaccharide) stabilizes fibrils against depolymerization at physiological pH (47,48). Moreover, the molecules tested in this study have all been shown to have no detectable effect on fibril appearance (see Fig. S2). Accordingly, for these fibril samples, at least, modification of membrane interactions can be assessed without interference from the effects of the small molecules on fibril assembly.

The results presented demonstrate that  $\beta_2m$  fibrils display distinct abilities to interact with, and disrupt, membranes when incubated with the different compounds assessed in this study. Particularly intriguing is the observation that incubation with small molecules belonging to similar structural and functional classes results in different membrane interactions with  $\beta_2m$  fibrils. Thus, although resveratrol did not inhibit membrane interactions of  $\beta_2m$  fibrillar aggregates, EGCG and bromophenol blue hampered membrane disruption, presumably by binding to the fibrillar aggregates and impeding their association with lipid bilayer, rather than by membrane stabilization mediated by the polyphenol molecules themselves.

The potency of the three polyphenols tested here to prevent lipid bilayer disruption is distributed in the following order:

EGCG > bromophenol blue > resveratrol.

These differences can be attributed to the distinct structural properties of the assessed compounds. EGCG, the most efficient inhibitor among the three polyphenols, has a  $pK_a$  value of 7.75 (Table 1). At the pH used in this study (pH 7.4), a significant fraction of EGCG molecules is negatively charged, which presumably mediates favorable electrostatic interactions with  $\beta_2m$  fibrils. Resveratrol, which did not alter lipid interactions of the fibrils, has a higher  $pK_a$  of 9.15 (Table 1), remaining nonionized under the same conditions. Further examination of the structures reveals that EGCG can form the largest number of hydrogen bonds of the three polyphenol compounds studied (11 bonds, Table 1), whereas resveratrol is able to make only three such bonds. Bromophenol blue, which demonstrated moderate inhibitory activity on membrane interactions of  $\beta_2m$  fibrils, is fully charged at pH 7.4 ( $pK_a$  3.5, Table 1); however, this molecule can form an intermediate amount of hydrogen bonds (five bonds, Table 1) compared with the other polyphenols studied here. EGCG is also the most hydrophilic polyphenol examined, as judged by its low partition coefficient between octanol and water ( $Log_D$ , Table 1). Together, these results suggest that electrostatic interactions and hydrogen bonding, rather than hydrophobic forces per se, are important determinants that govern the association of the polyphenols with  $\beta_2m$  fibrils and, thereby, attenuate membrane disruption by these fibrillar aggregates. When

comparing EGCG and bromophenol blue with a GAG of similar molecular weight (heparin disaccharide), it is evident that the latter failed to inhibit membrane activity of  $\beta_2m$  fibrils despite having a substantial number of negatively charged substituents and potentially more hydrogen-bond donors and acceptors than the polyphenols studied here (Table 1). Our findings imply that a combination of hydrophobic/aromatic interactions with electrostatic and hydrogen bonds is required for sequestering  $\beta_2m$  fibrillar aggregates by these small molecules. Neither of these factors alone is sufficient to rationalize the effect of polyphenols and heparin disaccharide on  $\beta_2m$  fibrils-membrane interactions.

Remarkable experimental outcomes were also found for fibrils incubated with heparin and its building unit, heparin disaccharide. Full-length heparin was found to be the most powerful inhibitor of  $\beta_2m$  fibril-induced damage of model membranes among all of the compounds tested. Unlike the small molecules, heparin abolished membrane disruption by  $\beta_2m$  fibrils and was able to disperse the large fibrillar aggregates observed at neutral pH. The inhibitory activity of heparin can be ascribed to efficient binding of its multiple negatively-charged sulfated and carboxylic units to  $\beta_2m$  fibrils that presumably impede their electrostatic interactions with negatively charged lipids. The remarkable difference in inhibitory potency of heparin and heparin disaccharide highlights the crucial role of the higher local concentration of functional groups in promoting interactions between the compound of interest and the  $\beta_2m$  amyloid fibrils. Thus, water-soluble polymers decorated by species possessing the ability to suppress membrane damage by amyloid aggregates may provide a promising strategy in the quest to design potent inhibitors of cell membrane disruption by amyloid fibrils. Interestingly in this regard, application of polymeric compounds conjugated to functional components such as fluorine or metal-chelating groups has been shown to impair the amyloidogenesis and cytotoxicity mediated by A $\beta$  peptide (34,37). Finally, and importantly, comparison of the results of fluorescence spectroscopy assays reporting upon lipid dynamics with those of membrane damage, visualized by dye release, fluorescence microscopy, and cryo-TEM, suggests that heparin modulates, rather than eliminates,  $\beta_2m$  fibril-membrane association.

In conclusion, the spectroscopic and microscopic data presented underscore the significant and divergent effects of the different fibril modulators tested upon membrane interactions of  $\beta_2m$  fibrils. Additional studies are required to assess whether our findings have a generic nature and are pertinent to other amyloidogenic proteins. In light of the emerging realization concerning the significance of membrane interactions upon the pathological profiles in protein misfolding diseases (3,19,60), the results suggest that an important facet of any study to develop inhibitors of amyloid diseases is the inclusion of analysis of the effect of potential inhibitors on amyloid-lipid interactions.

## SUPPORTING MATERIAL

Methods section, one table, and five figures are available at [http://www.biophysj.org/biophysj/supplemental/S0006-3495\(13\)00693-0](http://www.biophysj.org/biophysj/supplemental/S0006-3495(13)00693-0).

We thank Dr. Yael Kalissman (Ilse Katz Institute for Nano-Scale Science and Technology) for excellent technical assistance with cryo-EM experiments, Dr. Paul Beales (University of Leeds), and members of our laboratories for many helpful discussions.

T.S. was supported by the Marie Curie Intra-European Fellowship (No. 276621). We also acknowledge the Wellcome Trust (grants No. 075675 and No. 080707/z/06/z), the Biotechnology and Biological Sciences Research Council (grant No. BB/526502/1), and the British Council (BIRAX award) for funding this project.

## REFERENCES

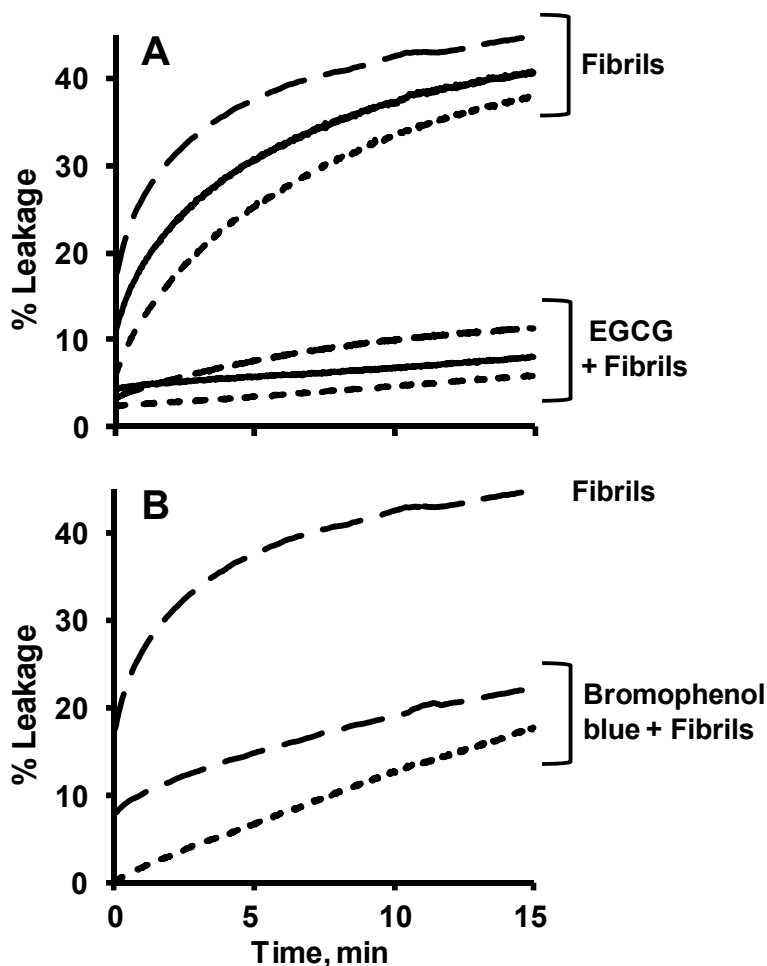
- Huang, Y., and L. Mucke. 2012. Alzheimer mechanisms and therapeutic strategies. *Cell*. 148:1204–1222.
- Meissner, W. G., M. Frasier, ..., E. Bezdard. 2011. Priorities in Parkinson's disease research. *Nat. Rev. Drug Discov.* 10:377–393.
- Stefani, M. 2007. Generic cell dysfunction in neurodegenerative disorders: role of surfaces in early protein misfolding, aggregation, and aggregate cytotoxicity. *Neuroscientist*. 13:519–531.
- Campioni, S., B. Mannini, ..., F. Chiti. 2010. A causative link between the structure of aberrant protein oligomers and their toxicity. *Nat. Chem. Biol.* 6:140–147.
- Ladiwala, A. R., J. Litt, ..., P. M. Tessier. 2012. Conformational differences between two amyloid  $\beta$  oligomers of similar size and dissimilar toxicity. *J. Biol. Chem.* 287:24765–24773.
- Caughey, B., and P. T. Lansbury. 2003. Protofibrils, pores, fibrils, and neurodegeneration: separating the possible protein aggregates from the innocent bystanders. *Annu. Rev. Neurosci.* 26:267–298.
- Winner, B., R. Jappelli, ..., R. Riek. 2011. In vivo demonstration that  $\alpha$ -synuclein oligomers are toxic. *Proc. Natl. Acad. Sci. USA*. 108:4194–4199.
- Bucciantini, M., E. Giannoni, ..., M. Stefani. 2002. Inherent toxicity of aggregates implies a common mechanism for protein misfolding diseases. *Nature*. 416:507–511.
- Cheng, I. H., K. Searce-Levie, ..., L. Mucke. 2007. Accelerating amyloid- $\beta$  fibrillization reduces oligomer levels and functional deficits in Alzheimer disease mouse models. *J. Biol. Chem.* 282:23818–23828.
- Pieri, L., K. Madiona, ..., R. Melki. 2012. Fibrillar  $\alpha$ -synuclein and huntingtin exon 1 assemblies are toxic to the cells. *Biophys. J.* 102:2894–2905.
- Xue, W. F., A. L. Hellewell, ..., S. E. Radford. 2009. Fibril fragmentation enhances amyloid cytotoxicity. *J. Biol. Chem.* 284:34272–34282.
- Okada, T., K. Ikeda, ..., K. Matsuzaki. 2008. Formation of toxic A $\beta$  (1–40) fibrils on GM1 ganglioside-containing membranes mimicking lipid rafts: polymorphisms in A $\beta$ (1–40) fibrils. *J. Mol. Biol.* 382:1066–1074.
- Xue, W. F., A. L. Hellewell, ..., S. E. Radford. 2010. Fibril fragmentation in amyloid assembly and cytotoxicity: when size matters. *Prion*. 4:20–25.
- Ren, P. H., J. E. Lauckner, ..., R. R. Kopito. 2009. Cytoplasmic penetration and persistent infection of mammalian cells by polyglutamine aggregates. *Nat. Cell Biol.* 11:219–225.
- Luk, K. C., V. Kehm, ..., V. M. Lee. 2012. Pathological  $\alpha$ -synuclein transmission initiates Parkinson-like neurodegeneration in nontransgenic mice. *Science*. 338:949–953.
- Li, J. Y., E. Englund, ..., P. Brundin. 2008. Lewy bodies in grafted neurons in subjects with Parkinson's disease suggest host-to-graft disease propagation. *Nat. Med.* 14:501–503.
- Cremades, N., S. I. Cohen, ..., D. Klenerman. 2012. Direct observation of the interconversion of normal and toxic forms of  $\alpha$ -synuclein. *Cell*. 149:1048–1059.
- Martins, I. C., I. Kuperstein, ..., F. Rousseau. 2008. Lipids revert inert A $\beta$  amyloid fibrils to neurotoxic protofibrils that affect learning in mice. *EMBO J.* 27:224–233.
- Auluck, P. K., G. Caraveo, and S. Lindquist. 2010.  $\alpha$ -Synuclein: membrane interactions and toxicity in Parkinson's disease. *Annu. Rev. Cell Dev. Biol.* 26:211–233.
- Jelinek, R. 2011. Lipids and Cellular Membranes in Amyloid Diseases. Wiley-VCH, Weinheim, Germany.
- Pithadia, A. S., A. Kochi, ..., M. H. Lim. 2012. Reactivity of diphenylpropynone derivatives toward metal-associated amyloid- $\beta$  species. *Inorg. Chem.* 51:12959–12967.
- Cheng, P. N., C. Liu, ..., J. S. Nowick. 2012. Amyloid  $\beta$ -sheet mimics that antagonize protein aggregation and reduce amyloid toxicity. *Nat. Chem.* 4:927–933.
- Hård, T., and C. Lendel. 2012. Inhibition of amyloid formation. *J. Mol. Biol.* 421:441–465.
- Han, Y. S., W. H. Zheng, ..., R. Quirion. 2004. Neuroprotective effects of resveratrol against  $\beta$ -amyloid-induced neurotoxicity in rat hippocampal neurons: involvement of protein kinase C. *Br. J. Pharmacol.* 141:997–1005.
- Evers, F., C. Jeworrek, ..., R. Winter. 2009. Elucidating the mechanism of lipid membrane-induced IAPP fibrillogenesis and its inhibition by the red wine compound resveratrol: a synchrotron x-ray reflectivity study. *J. Am. Chem. Soc.* 131:9516–9521.
- Rezaei-Zadeh, K., G. W. Arendash, ..., J. Tan. 2008. Green tea epigallocatechin-3-gallate (EGCG) reduces  $\beta$ -amyloid mediated cognitive impairment and modulates tau pathology in Alzheimer transgenic mice. *Brain Res.* 1214:177–187.
- Ehrnhoefer, D. E., M. Duennwald, ..., E. E. Wanker. 2006. Green tea (–)epigallocatechin-gallate modulates early events in huntingtin misfolding and reduces toxicity in Huntington's disease models. *Hum. Mol. Genet.* 15:2743–2751.
- Ehrnhoefer, D. E., J. Bieschke, ..., E. E. Wanker. 2008. EGCG redirects amyloidogenic polypeptides into unstructured, off-pathway oligomers. *Nat. Struct. Mol. Biol.* 15:558–566.
- Ladiwala, A. R., J. C. Lin, ..., P. M. Tessier. 2010. Resveratrol selectively remodels soluble oligomers and fibrils of amyloid A $\beta$  into off-pathway conformers. *J. Biol. Chem.* 285:24228–24237.
- Meng, F., A. Abedini, ..., D. P. Raleigh. 2010. The flavanol (–)epigallocatechin 3-gallate inhibits amyloid formation by islet amyloid polypeptide, disaggregates amyloid fibrils, and protects cultured cells against IAPP-induced toxicity. *Biochemistry*. 49:8127–8133.
- Lever, R., and C. P. Page. 2002. Novel drug development opportunities for heparin. *Nat. Rev. Drug Discov.* 1:140–148.
- Bravo, R., M. Arimon, ..., X. Fernández-Busquets. 2008. Sulfated polysaccharides promote the assembly of amyloid  $\beta$  (1–42) peptide into stable fibrils of reduced cytotoxicity. *J. Biol. Chem.* 283:32471–32483.
- Pérez, M., F. Wandosell, ..., J. Avila. 1998. Sulphated glycosaminoglycans prevent the neurotoxicity of a human prion protein fragment. *Biochem. J.* 335:369–374.
- Liu, G., P. Men, ..., M. A. Smith. 2009. Nanoparticle-chelator conjugates as inhibitors of amyloid- $\beta$  aggregation and neurotoxicity: a novel therapeutic approach for Alzheimer disease. *Neurosci. Lett.* 455:187–190.
- Mannini, B., R. Cascella, ..., F. Chiti. 2012. Molecular mechanisms used by chaperones to reduce the toxicity of aberrant protein oligomers. *Proc. Natl. Acad. Sci. USA*. 109:12479–12484.
- Ladiwala, A. R., M. Bhattacharya, ..., P. M. Tessier. 2012. Rational design of potent domain antibody inhibitors of amyloid fibril assembly. *Proc. Natl. Acad. Sci. USA*. 109:19965–19970.

37. Saraiva, A. M., I. Cardoso, ..., G. Brezesinski. 2010. Controlling amyloid- $\beta$  peptide(1-42) oligomerization and toxicity by fluorinated nanoparticles. *ChemBioChem*. 11:1905–1913.
38. Högen, T., J. Levin, ..., A. Giese. 2012. Two different binding modes of  $\alpha$ -synuclein to lipid vesicles depending on its aggregation state. *Biophys. J.* 102:1646–1655.
39. Burmeister, W. P., L. N. Gastinel, ..., P. J. Bjorkman. 1994. Crystal structure at 2.2 Å resolution of the MHC-related neonatal Fc receptor. *Nature*. 372:336–343.
40. Bellotti, V., M. Stoppini, ..., G. Ferri. 1998.  $\beta$ 2-microglobulin can be refolded into a native state from ex vivo amyloid fibrils. *Eur. J. Biochem*. 258:61–67.
41. Porter, M. Y., K. E. Routledge, ..., E. W. Hewitt. 2011. Characterization of the response of primary cells relevant to dialysis-related amyloidosis to  $\beta$ 2-microglobulin monomer and fibrils. *PLoS ONE*. 6:e27353.
42. Stevenson, D. E., and R. D. Hurst. 2007. Polyphenolic phytochemicals—just antioxidants or much more? *Cell. Mol. Life Sci.* 64:2900–2916.
43. Jones, C. J., S. Beni, ..., C. K. Larive. 2011. Heparin characterization: challenges and solutions. *Annu. Rev. Anal. Chem.* 4:439–465.
44. Moscho, A., O. Orwar, ..., R. N. Zare. 1996. Rapid preparation of giant unilamellar vesicles. *Proc. Natl. Acad. Sci. USA*. 93:11443–11447.
45. Parisio, G., A. Marini, ..., B. Mennucci. 2011. Polarity-sensitive fluorescent probes in lipid bilayers: bridging spectroscopic behavior and microenvironment properties. *J. Phys. Chem. B*. 115:9980–9989.
46. Bazar, E., and R. Jelinek. 2010. Divergent heparin-induced fibrillation pathways of a prion amyloidogenic determinant. *ChemBioChem*. 11:1997–2002.
47. Myers, S. L., S. Jones, ..., S. E. Radford. 2006. A systematic study of the effect of physiological factors on  $\beta$ 2-microglobulin amyloid formation at neutral pH. *Biochemistry*. 45:2311–2321.
48. Yamamoto, S., I. Yamaguchi, ..., H. Naiki. 2004. Glycosaminoglycans enhance the trifluoroethanol-induced extension of  $\beta$  2-microglobulin-related amyloid fibrils at a neutral pH. *J. Am. Soc. Nephrol*. 15:126–133.
49. Chen, R. F., and J. R. Knutson. 1988. Mechanism of fluorescence concentration quenching of carboxyfluorescein in liposomes: energy transfer to nonfluorescent dimers. *Anal. Biochem*. 172:61–77.
50. White, H. E., J. L. Hodgkinson, ..., H. R. Saibil. 2009. Globular tetramers of  $\beta$  (2)-microglobulin assemble into elaborate amyloid fibrils. *J. Mol. Biol.* 389:48–57.
51. Larsen, J., N. S. Hatzakis, and D. Stamou. 2011. Observation of inhomogeneity in the lipid composition of individual nanoscale liposomes. *J. Am. Chem. Soc.* 133:10685–10687.
52. Han, Y. S., S. Bastianetto, ..., R. Quirion. 2006. Specific plasma membrane binding sites for polyphenols, including resveratrol, in the rat brain. *J. Pharmacol. Exp. Ther.* 318:238–245.
53. Sun, Y., W. C. Hung, ..., H. W. Huang. 2009. Interaction of tea catechin (–)-epigallocatechin gallate with lipid bilayers. *Biophys. J.* 96:1026–1035.
54. Milanese, L., T. Sheynis, ..., H. R. Saibil. 2012. Direct three-dimensional visualization of membrane disruption by amyloid fibrils. *Proc. Natl. Acad. Sci. USA*. 109:20455–20460.
55. Pebay-Peyroula, E., E. J. Dufourc, and A. G. Szabo. 1994. Location of diphenyl-hexatriene and trimethylammonium-diphenyl-hexatriene in dipalmitoylphosphatidylcholine bilayers by neutron diffraction. *Biophys. Chem.* 53:45–56.
56. Rodrigues, C., P. Gameiro, ..., B. de Castro. 2003. Interaction of rifampicin and isoniazid with large unilamellar liposomes: spectroscopic location studies. *Biochim. Biophys. Acta*. 1620:151–159.
57. Vilasi, S., R. Sarcina, ..., I. Sirangelo. 2011. Heparin induces harmless fibril formation in amyloidogenic W7FW14F apomyoglobin and amyloid aggregation in wild-type protein in vitro. *PLoS ONE*. 6:e22076.
58. Sciacca, M. F., S. A. Kotler, ..., A. Ramamoorthy. 2012. Two-step mechanism of membrane disruption by A $\beta$  through membrane fragmentation and pore formation. *Biophys. J.* 103:702–710.
59. Woods, L. A., G. W. Platt, ..., S. E. Radford. 2011. Ligand binding to distinct states diverts aggregation of an amyloid-forming protein. *Nat. Chem. Biol.* 7:730–739.
60. Williams, T. L., and L. C. Serpell. 2011. Membrane and surface interactions of Alzheimer's A $\beta$  peptide—insights into the mechanism of cytotoxicity. *FEBS J.* 278:3905–3917.
61. SciFinder. 2013. Physical properties of molecules used in the study <http://www.scifinder.cas.org/scifinder/view/scifinder/scifinderExplore.jsf> Accessed January 2013.

## Supporting Material

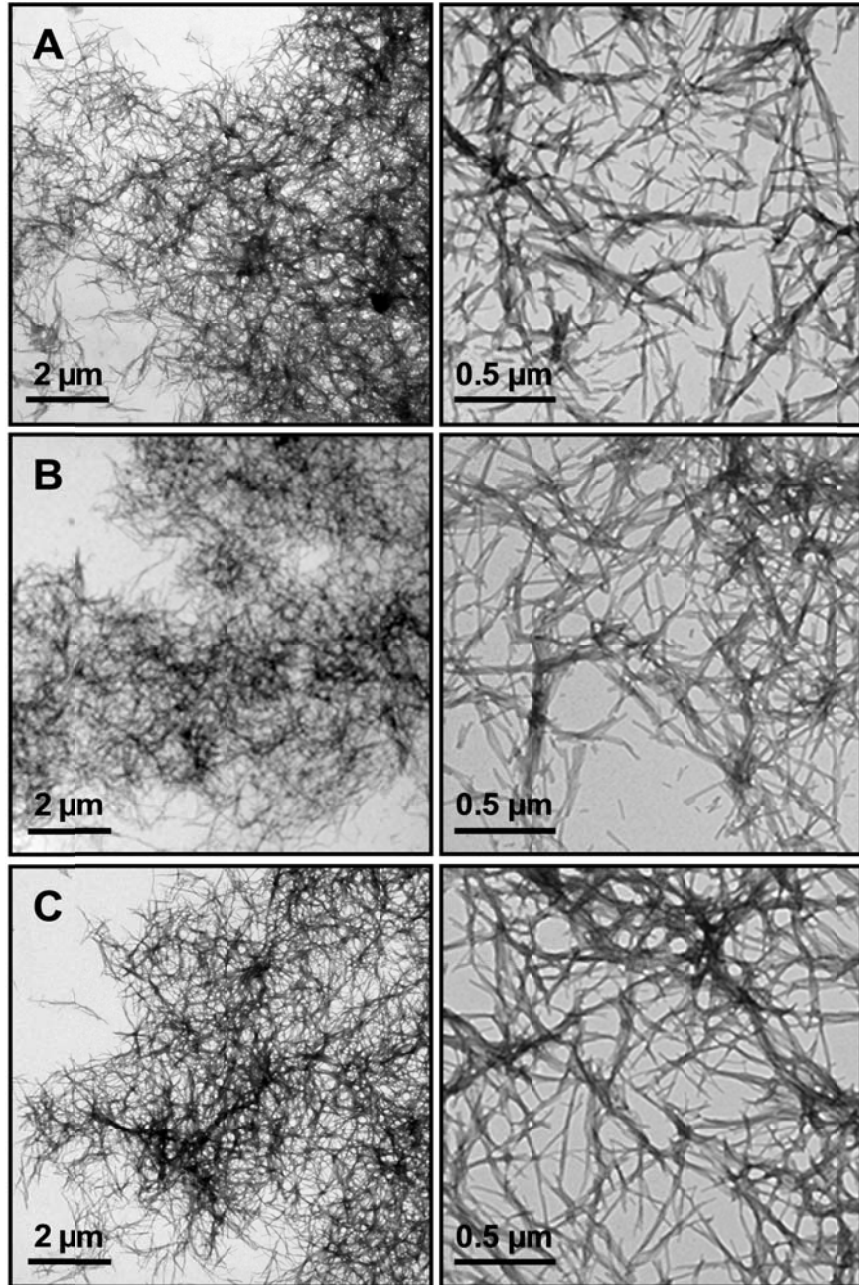
### Aggregation modulators interfere with membrane interactions of $\beta_2$ -microglobulin fibrils

Tania Sheynis<sup>1,2\*</sup>, Anat Friediger<sup>1\*</sup>, Wei-Feng Xue<sup>2,3</sup>, Andrew L. Hellewell<sup>2</sup>, Kevin W. Tipping<sup>2</sup>, Eric W. Hewitt<sup>2</sup>, Sheena E. Radford<sup>2</sup>, Raz Jelinek<sup>1</sup>



**Figure S1: The effect of longer pre-incubation of polyphenols with  $\beta_2$ m fibrils on the fibril-induced vesicle leakage.**  $\beta_2$ m fibrils were incubated in pH 7.4 buffer (A-B) alone; with (A) EGCG or (B) bromophenol blue for the following time periods: *Long dash*: 3min; *solid*: 15 min; *short dash*: 30 min.

Prolonged incubation of  $\beta_2$ m fibrils in pH 7.4 buffer with no additives reduced the extent of vesicle leakage by  $\sim 7\%$  relative to the 3 min incubation, presumably due to formation of larger fibrillar aggregates at this pH [52]. Fibrils treated with either EGCG or bromophenol blue for 30 min gave rise to comparable reduction of the extent of dye leakage. Thus, the longer incubation time does not improve the inhibitory properties of these polyphenols.



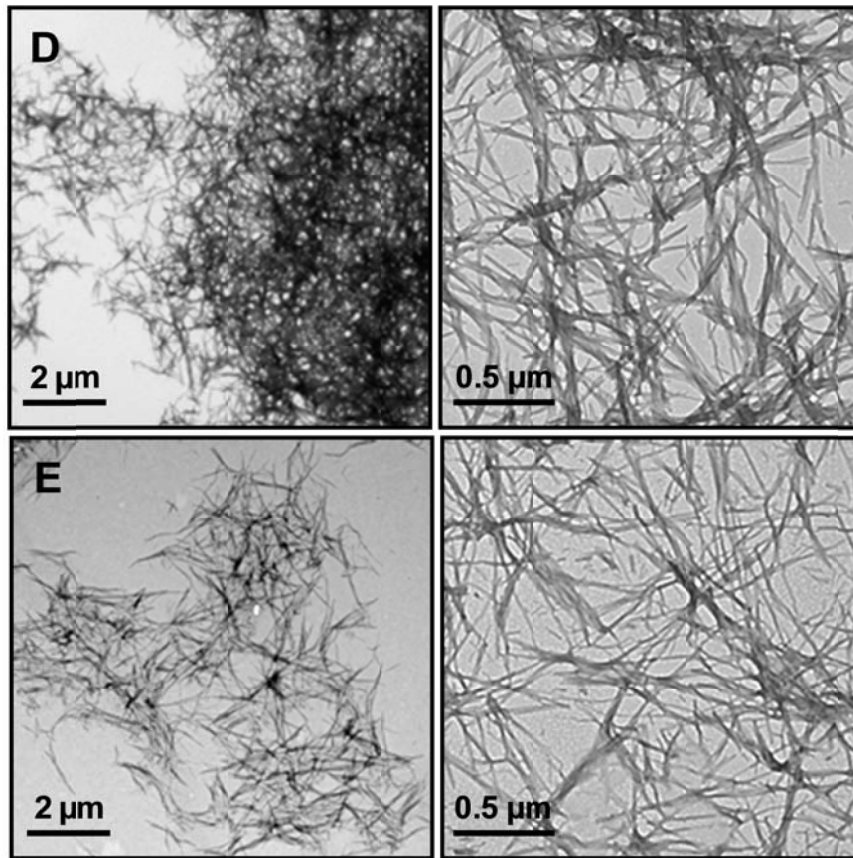


**Figure S2: TEM images of  $\beta_2m$  fibrils incubated with polyphenols and GAGs in the absence of lipid vesicles. (A)  $\beta_2m$  fibrils in pH 7.4 buffer (control);  $\beta_2m$  fibrils incubated for 5 min with (B) EGCG; (C) bromophenol blue; (D) resveratrol or (E) full-length heparin. Each image is shown on two different scales.**

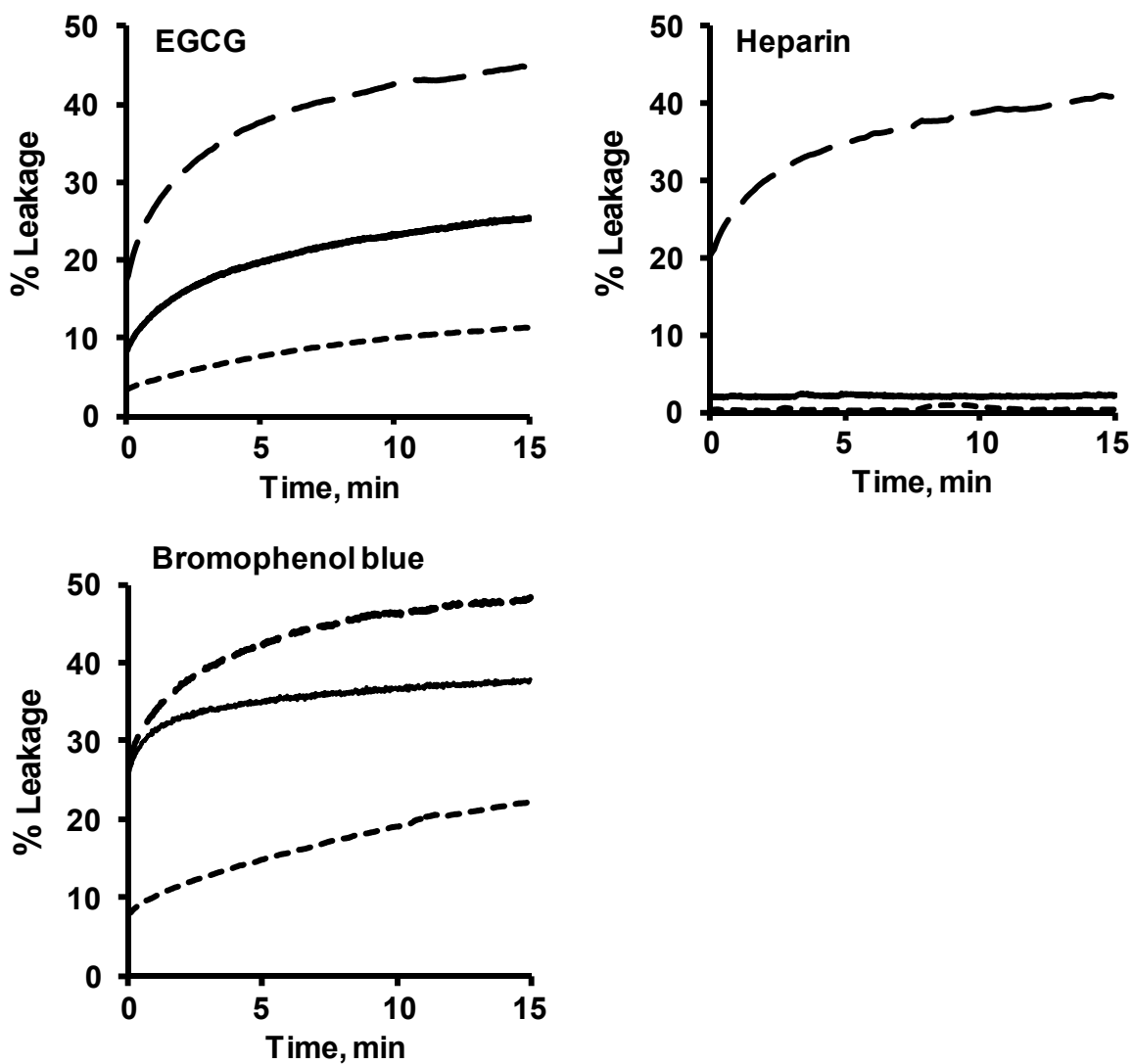


**Figure S3: Kinetic curves showing the effect of vesicle pre-incubation with different additives on  $\beta_2$ m-fibril induced membrane leakage. *Long dashed*:  $\beta_2$ m fibrils alone (no fibrillation modulators added). *Solid line*: fibrillation modulators incubated with vesicles for 30 min before addition of fibrils. *Short dashed*: fibrillation modulators incubated with  $\beta_2$ m fibrils for 3 min prior to addition to the vesicles.**

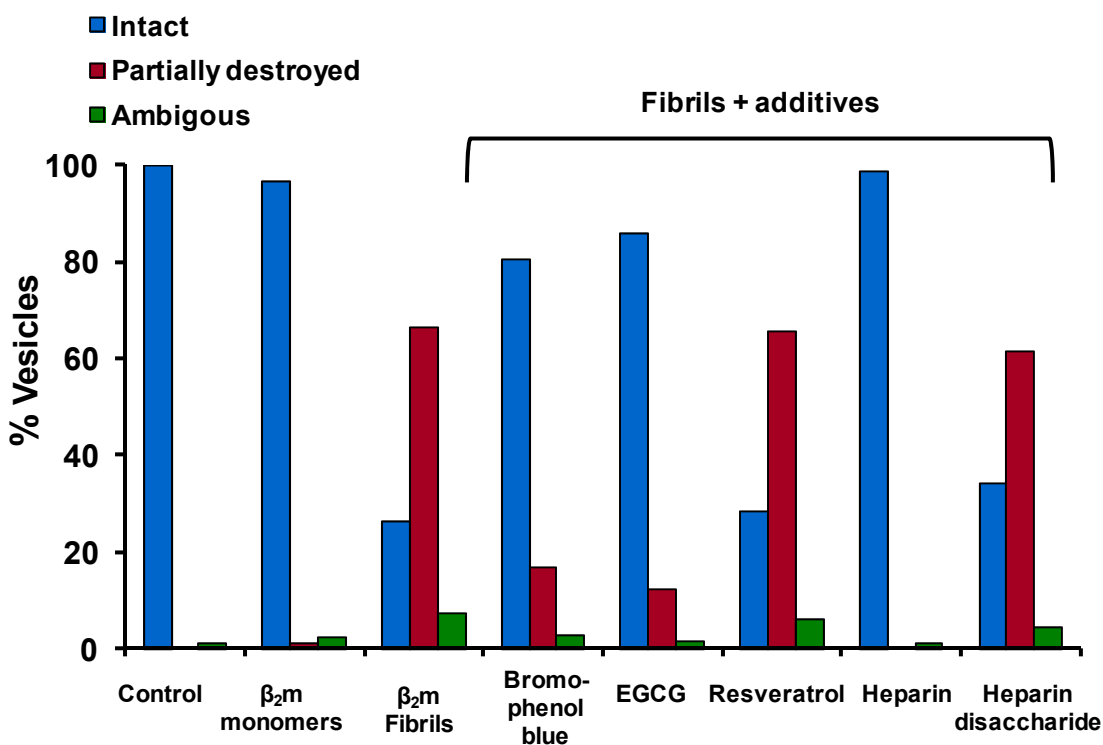


**Figure S4: Counting statistics of GV distortion by  $\beta_2m$  fibrils and the effect of different additives.** GV counting was acquired from confocal images (representative data are shown in Fig. 3) for the following samples: GVs in buffer (control), GVs incubated with:  $\beta_2m$  monomers;  $\beta_2m$  fibrils or fibril/additives mixtures. Total number of vesicles counted in each category is indicated in Table S1. Vesicles were classified as intact; partially destroyed (exhibiting remaining spherical structure as in Fig. 3D(i)) or ambiguous (GVs that appeared in close proximity to fibrillar aggregates and thus could not be reliably ascribed to either intact or partially destroyed). Note that completely disintegrated vesicles were not included in these counts since it is difficult to estimate their quantity.



<b>Compound</b>	<b>Total vesicle counts</b>	<b>N of fibrillar aggregates coated by lipids</b>
<b>Control (vesicles only)</b>	109	N/A
<b><math>\beta_2m</math> monomers</b>	90	N/A
<b><math>\beta_2m</math> fibrils</b>	95	39
<b>Bromophenol blue + fibrils</b>	108	15
<b>EGCG + fibrils</b>	122	7
<b>Resveratrol + fibrils</b>	81	29
<b>Heparin + fibrils</b>	90	0
<b>Heparin disaccharide + fibrils</b>	88	36

**Table S1: Counting statistics of GV disintegration by  $\beta_2m$  fibrils.** GV and fibrillar aggregates counts were acquired from confocal images (representative data are shown in Fig. 3). Only fibrillar aggregates coated by lipids but not bound to vesicles were taken into account (examples are shown in Fig. 3D(ii) by arrows). Note that lipids extracted by a fibrillar aggregate could be derived from a single or multiple vesicles. Note that completely destroyed GVs were not included in total vesicle counts.

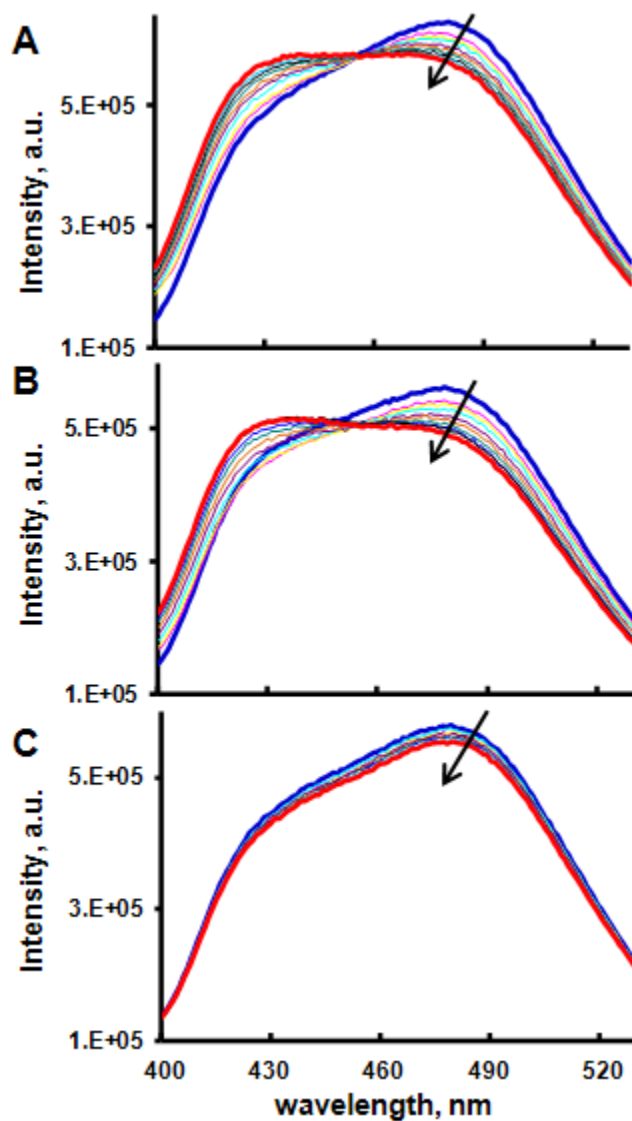


**Figure S5: Time course of Laurdan fluorescence shift.** Emission spectra of Laurdan within PC/PG (1/1) LUVs were recorded over 20 min after addition of the following compounds to the vesicles: **(A)**  $\beta_2m$  fibrils; **(B)**  $\beta_2m$  fibrils pre-incubated for 3 min with full length heparin; **(C)**  $\beta_2m$  monomers. Arrows indicate time progression at the following intervals: 0, 0.5, 1, 2, 4, 7, 10, 13, 16 and 20 min. The first and the last time points are highlighted in blue and red, respectively.

## Supporting Methods

### Transmission Electron Microscopy (TEM).

$\beta_2m$  fibrils were incubated with polyphenols and GAGs in the absence of vesicles as follows. Aliquots from  $\beta_2m$  fibril stock solution (120  $\mu$ M monomer equivalent concentration) were incubated for 3 min with the required amount of the tested compound to obtain the following  $\beta_2m$ -to-inhibitor ratios:  $\beta_2m$ /heparin - 1:0.4 (*w/w*);  $\beta_2m$ /polyphenols (EGCG, bromophenol blue, resveratrol) – 1:1 (*w/w*). The samples were then diluted 10-fold by the liposome buffer (pH 7.4) and further incubated for 5 min prior to deposition on 300 mesh copper grids covered by a carbon-stabilized Formvar film. Following 30 sec incubation, excess solutions were removed and the grids were negatively stained for 20 sec with a 1 % (*w/v*) uranyl acetate solution. For the control sample, the liposome buffer was used instead of inhibitors. Samples were viewed with a FEI Tecnai G2 F20 field emission gun (FEG) electron microscope, and the images were recorded using Gatan Ultrascan 4000 CCD camera at 120 kV.

### Preparation of rhodamine-labeled $\beta_2m$ monomer:

The fluorescent dye 5-(and-6)- carboxytetramethylrhodamine-SE (TMR) was dissolved in DMSO at 1 mg/ml and added dropwise to a stirred  $\beta_2m$  solution (10 mg/ml of protein in 10 mM sodium bicarbonate buffer, pH 9.4) in the dark for 1 hour. A ten-fold molar excess of the dye over  $\beta_2m$  was used. A PD10 desalting column (GE Healthcare, Little Chalfont, UK) was equilibrated using 25 ml of 100 mM Tris-HCl pH 8.0. Subsequently, 2.5 ml of the TMR- $\beta_2m$  conjugate was loaded onto the column and eluted using 3.5 ml of 100 mM Tris-HCl, pH 8.0. The TMR-labelled  $\beta_2m$  was dialyzed against double-distilled water, lyophilized and stored at -20 °C. The protein was labelled with 2, 3, 4 or 5 TMR molecules per monomer with a ratio of ~1:2:2:1 as determined by ESI-MS. TMR-labelled fibrils were prepared by mixing unlabeled and labeled monomers such that the final preparation contained 10% of TMR-bound monomer.

### Preparation of Large Unilamellar Vesicles (LUVs):

The egg PC/PG 1/1 (molar ratio) lipid mixture was supplemented with 0.24 % (molar ratio) of rhodamine-PE for determination of lipid concentration. All lipid components were dissolved in chloroform/ethanol (1:1, *v/v*) and dried together *in vacuo* for 4 hours. The resulting lipid films were hydrated in the liposome buffer (50 mM Hepes, 110 mM NaCl, 1 mM EDTA, 0.02 % (*w/v*)  $\text{NaN}_3$ , pH 7.4) by vortexing lipid samples for 2 hours. LUVs were prepared by extruding the lipid suspensions through a polycarbonate filter with 400 nm pore size and annealing for 30 min at room temperature. The vesicles were stored at +4 °C and used within 1 day.